

Thermodynamic phases in first detected return times of quantum many-body systems

Benjamin Walter,¹ Gabriele Perfetto,² and Andrea Gambassi³

¹*Department of Mathematics, Imperial College London, London SW7 2AZ, United Kingdom*

²*Institut für Theoretische Physik, Universität Tübingen,*

Auf der Morgenstelle 14, 72076 Tübingen, Germany

³*SISSA–International School for Advanced Studies and INFN, via Bonomea 265, 34136 Trieste, Italy*

We study the probability distribution of the first return time to the initial state of a quantum many-body system subject to stroboscopic projective measurements. We show that this distribution can be interpreted as a continuation of the canonical partition function of a classical spin chain with non-interacting domains at equilibrium, which is entirely characterised by the Loschmidt amplitude of the quantum many-body system. This allows us to conclude that this probability may decay either algebraically or exponentially at long times, depending on whether the spin model displays a ferromagnetic or a paramagnetic phase. We illustrate this idea on the example of the return time of N adjacent fermions in a tight-binding model, revealing a rich phase behaviour, which can be tuned by scaling the probing time as a function of N . The analysis presented here provides an overarching understanding of many-body quantum first-detection problems in terms of equilibrium thermodynamic phases. Our theoretical predictions turn out to be in excellent agreement with exact numerical computations.

Introduction— Measurements in quantum mechanics result in intrinsically stochastic outcomes and affect the quantum state [1–4]. In particular, the first time at which a quantum state $|\Psi(t)\rangle$ is detected in a certain target state $|\Psi_T\rangle$ is a stochastic quantity of fundamental interest [5, 6], which depends on the measurement protocol. Recently, the probability of this first detection time under successive projective measurements has been studied extensively [7–27]. For a single quantum particle hopping on a line and subject to measurements at stroboscopic times $\tau, 2\tau, 3\tau, \dots$, the probability F_k of first detection at time $k\tau$ at a certain position shows high sensitivity to the probing time τ [12–16], the quantum Zeno effect [28, 29] as $\tau \rightarrow 0$, and a rich behaviour depending on the position of the target state. Moreover, it displays a long-time universal behavior $F_k \sim k^{-3}$ [12, 13, 15] unlike its classical equivalent of the first-passage time [30]. All these studies treat single-particle systems. For quantum many-body systems, instead, analytical results have been recently obtained only for mean values [31]. For the first-detection distribution results are limited to small system sizes [32, 33] due to the exponential complexity of many-body numerical simulations. No analytical results valid for an arbitrary number of particle are currently available.

In this work, we address this problem by deriving exact analytical results in the case of the many-body first detected return time (FDRT), where the initial state coincides with the target state $|\Psi_T\rangle = |\Psi(0)\rangle$. We do so by developing a general and exact mapping of the quantum many-body FDRT probability F_k onto the classical partition function of a one-dimensional spin model with non-interacting domains [34–41]. Similar classical partition functions appear in studies of the DNA melting transitions [34–37] or in non-equilibrium currents [41]. This mapping allows us to classify the different asymptotic decays of F_k as a function of k in terms of the equilibrium

phases of that classical partition function. Namely, we show that an algebraic decay corresponds to a ferromagnetic behavior, where large spin domains/long intervals of measurement-free evolution dominate F_k . On the contrary, an exponential decay of F_k is found to correspond to the paramagnetic (disordered) phase of the classical spin model, where short domains/short measurement-free time intervals are relevant. We illustrate this approach by considering the case of N adjacent fermions in a tight-binding model, which for $N = 1$ reduces to previous studies [12, 13]. For finite N , we map this model onto the ferromagnetic phase of the truncated inverse-distance square Ising model [38–40, 42] and we exactly determine the asymptotic algebraic decay exponent c_N of $F_k \sim k^{-2c_N}$. For $N = \infty$, instead, F_k decays exponentially upon increasing k , which maps to paramagnetic behavior. Crucially, for finite N , we show that a crossover occurs from the aforementioned paramagnetic-exponential decay to a ferromagnetic-algebraic one. The corresponding crossover time increases upon increasing the number N of particles, an inherent feature of the quantum ballistic many-body nature of the dynamics. This crucially allows one to tune the onset of the algebraic decay of F_k to more accessible short times. Our analytical predictions provide significant steps forward in the direction of connecting behavior of non-equilibrium quantum fluctuations to that of equilibrium thermodynamic phases.

First detected return— We study the FDRT probability of many-body systems described by a Hamiltonian \mathcal{H} , with associated unitary evolution $U(t) = e^{-i\mathcal{H}t}$. This problem can be tackled by extending the formalism developed in Refs. [8, 9, 12, 13] to the many-body realm, see Fig. 1(a). Right before the first measurement at time τ , the overlap of the wavefunction $|\Psi(\tau^-)\rangle = U(\tau)|\Psi(0)\rangle$ with the target state $|\Psi(0)\rangle$ is given by the Loschmidt

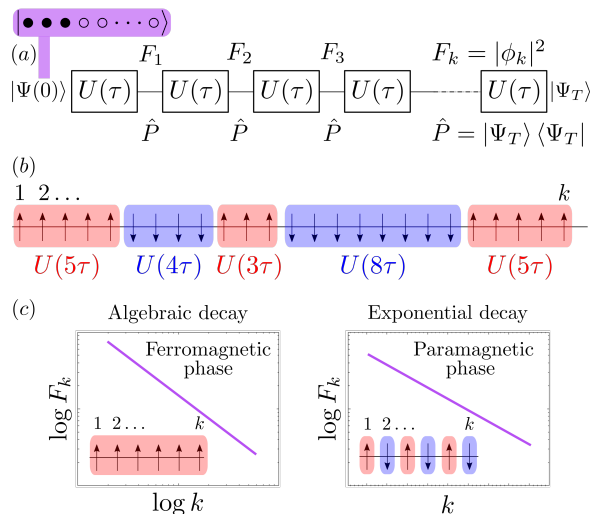


FIG. 1. **Quantum many-body first detection time.** (a) A wavefunction evolves with unitary dynamics $U(\tau)$ interspersed by projective measurements \hat{P} occurring at stroboscopic times multiples of τ . The target state $|\Psi_T\rangle = |\Psi(0)\rangle$ is first detected at the k th measurement with first detected return amplitude ϕ_k and probability $F_k = |\phi_k|^2$. The protocol terminates at the first successful detection in $|\Psi_T\rangle$. (b) ϕ_k can be decomposed in terms of time intervals of measurements-free dynamics $U(n\tau)$ (in the figure $n = 5, 4, 3, 8$ and 5 , from left to right). Each interval can be mapped into a domain of aligned classical spins, with spins interacting via long-range interactions. Accordingly, ϕ_k is mapped onto a problem of statistical mechanics of domains at equilibrium in a volume k . (c) When F_k is determined by long measurement-free intervals $\sim U(k\tau)$, one has a ferromagnetic phase and F_k decays algebraically upon increasing k . Conversely, when short intervals $\sim U(\tau)$ dominate, F_k decays exponentially. This corresponds to the paramagnetic phase.

amplitude

$$\mathcal{L}(\tau) = \langle \Psi(0) | U(\tau) | \Psi(0) \rangle, \quad (1)$$

and therefore the detection in $|\Psi(0)\rangle$ is successful with probability $F_1 = |\mathcal{L}(\tau)|^2$. In this case, one has $|\Psi(\tau^+)\rangle = |\Psi(0)\rangle$. If the detection is, instead, unsuccessful, the wavefunction is projected onto the space orthogonal to the target state and thus it reads $|\Psi(\tau^+)\rangle = (\mathbb{1} - \hat{P}) |\Psi(\tau^-)\rangle / \sqrt{1 - F_1}$, where $\hat{P} = |\Psi(0)\rangle \langle \Psi(0)|$, such that $\langle \Psi(\tau^+) | \Psi(\tau^+) \rangle = 1$. Until the next measurement, the state evolves unitarily as $|\Psi(t)\rangle = U(t - \tau) |\Psi(\tau^+)\rangle$ for $\tau < t < 2\tau$, whence the procedure is repeated until the first detection in the target state occurs. The overlap between the target state and the unnormalised wavefunction after $k - 1$ unsuccessful detections evolved until immediately before the k th measurement defines the *first detection amplitude*

$$\phi_k = \langle \Psi(0) | U(\tau) \left[(\mathbb{1} - \hat{P}) U(\tau) \right]^{k-1} | \Psi(0) \rangle. \quad (2)$$

The FDRT probability F_k is given by $F_k = |\phi_k|^2$. The generating function $\hat{\mathcal{L}}(z) = \sum_{k \geq 1} \phi_k z^k$ of ϕ_k is related to

that $\hat{\mathcal{L}}(z) = \sum_{k \geq 1} \mathcal{L}_k z^k$ of $\mathcal{L}_k \equiv \mathcal{L}(k\tau)$ by [8, 10, 12]

$$\hat{\phi}(z) = \frac{\hat{\mathcal{L}}(z)}{1 + \hat{\mathcal{L}}(z)}. \quad (3)$$

The ϕ_k 's are then determined as the integral

$$\phi_k = \oint \frac{dz}{2\pi i} \frac{\hat{\phi}(z)}{z^{k+1}}, \quad (4)$$

along a contour enclosing the origin $z = 0$ and within the domain of analyticity of $\hat{\phi}(z)$.

By expanding the $(k - 1)$ th power of $(\mathbb{1} - \hat{P})U(\tau)$ in Eq. (2), one finds that ϕ_k equals an alternating sum of measurement-free time intervals with evolution $U(\ell_r\tau)$ interspersed with r projections \hat{P} , i.e., of terms of the form $\langle \Psi(0) | U(\ell_1\tau) \hat{P} U(\ell_2\tau) \dots \hat{P} U(\ell_r\tau) | \Psi(0) \rangle$. Accordingly, one can write

$$\phi_k = \sum_{r=1}^k (-1)^{r+1} \sum_{\ell_1, \ell_2, \dots, \ell_r=1}^{\infty} \left(\prod_{j=1}^r \mathcal{L}_{\ell_j} \right) \delta_{\sum_{j=1}^r \ell_j, k}. \quad (5)$$

Equation (5) is crucial to map the problem into the partition function of a classical lattice spin model with non-interacting domains, as sketched in Fig. 1(b). A configuration of the spin model corresponds to a partition of the total volume k into r consecutive domains of lengths ℓ_1, \dots, ℓ_r , with $\ell_1 + \dots + \ell_r = k$ (see Fig. 1). To each domain, a length-dependent energy $E(\ell)$ is associated resulting from the possibly long-range interactions among the spins within the domain. The ‘‘Boltzmann weight’’ w is associated, instead, to each domain wall. The canonical partition function of this model with fixed volume k can be written as

$$Z(k, w) = \sum_{r=1}^k w^{r+1} \sum_{\ell_1, \ell_2, \dots, \ell_r=1}^{\infty} \left(\prod_{j=1}^r e^{-E(\ell_j)} \right) \delta_{\sum_{j=1}^r \ell_j, k}. \quad (6)$$

It is then apparent that Eq. (5) can be recovered from Eq. (6) by letting $w \rightarrow -1$ and by identifying the Loschmidt amplitude $\mathcal{L}_\ell = \mathcal{L}(\ell\tau)$ in time with the Boltzmann factor $e^{-E(\ell)}$ in space. Differently from the classical model, $E(\ell) = -\ln \mathcal{L}(\ell\tau)$ may now take complex values depending on the sign of \mathcal{L}_ℓ , while $w = -1$ implies a purely imaginary energetic cost associated to a domain wall; these differences give rise to interferences when summed over, reflecting the quantum nature of ϕ_k . The analogy extends to the fixed-pressure (grand canonical) ensemble. Summing over the length k , one obtains the partition function

$$\mathcal{Z}(z, w) = \sum_{k=1}^{\infty} z^k Z(k, w) = \frac{w^2 \hat{\mathcal{L}}(z)}{1 - w \hat{\mathcal{L}}(z)}, \quad (7)$$

where z is the exponential of the pressure conjugate to the volume k , while $\hat{\mathcal{L}}(z) = \sum_{k \geq 1} e^{-E(k)} z^k$ is the grand

canonical partition function of a single domain. Setting $w \rightarrow -1$ in Eq. (7), one recovers $\hat{\phi}(z)$ given in Eq. (3).

Emergence of phases— In the thermodynamic limit $k \rightarrow \infty$, the spin model introduced in Eq. (6) may exhibit, depending on the form of $E(\ell)$ and on the value of w , either a ferromagnetic or a paramagnetic phase [38–40, 42]. This may happen even in one spatial dimension since $E(\ell)$ results from possibly long-range interactions among the spins within the domain. In the former case, the equilibrium ensemble is dominated by a globally ordered spin domain of length $\ell \sim \mathcal{O}(k)$, while in the latter by disordered spins with $\ell \sim \mathcal{O}(1)$. Identifying $\hat{\phi}(z)$ as $\mathcal{Z}(z, w \rightarrow -1)$ allows us to establish the possibility of observing two different behaviours of ϕ_k at large k , as shown in Fig. 1(c). In fact, if the spin model is in the ferromagnetic phase, the dominant configuration is a single, extended domain and thus $Z(k, -1) \sim e^{-E(k)}$; according to the mapping, this corresponds to the leading term of the first-detection amplitude being $\phi_k \sim \mathcal{L}(k\tau)$. If the spin model is, instead, in the paramagnetic phase, and therefore it displays disordered domains, the partition function $Z(k, -1) \sim e^{-kE(1)}$ is dominated by many short domains. In terms of the quantum evolution, this corresponds to $\phi_k \sim [\mathcal{L}(\tau)]^k$ being dominated by the product over many Loschmidt amplitudes of short duration.

The two cases mentioned above are understood through the analytic properties of $\hat{\phi}(z) = \mathcal{Z}(z, -1)$ as a function of z , which determines ϕ_k according to Eq. (4). The radius of convergence of $\hat{\phi}$ is controlled by its singularity at $z = z^*$, which is closest to the origin. By inspection of Eqs. (3) and (7), the singular point z^* may arise from either (i) a root in the denominator, i.e., $1 + \hat{\mathcal{L}}(z^*) = 0$, leading to a simple pole or (ii) a non-analyticity in $\hat{\mathcal{L}}(z^*)$ leading to a branch point. If the singularity at z^* is a simple pole, $\hat{\phi}(z) \sim (z - z^*)^{-1}$, the integration in Eq. (4) renders $\phi_k \sim (z^*)^{-k}$ and therefore an exponential dependence of ϕ_k on k . This exponential decay corresponds to the configuration with k domains, i.e., to the paramagnetic phase. If the singularity z^* is due to a branch point, instead, $\hat{\phi}(z) \sim |z - z^*|^{c-1}$ and, via Tauberian theorems, one obtains an algebraic decay of $\phi_k \sim k^{-c}$ for large k [43]. Algebraic growth of a canonical partition function as a function of the volume is a consequence of a single domain in a long-range interacting spin model and thus we associate this behaviour with the ferromagnetic phase.

We illustrate this mapping by investigating the FDRT of N free fermions with Hamiltonian $\mathcal{H} = \sum_{j=-\infty}^{\infty} (c_j^\dagger c_{j+1} + c_{j+1}^\dagger c_j)$, where c_j (c_j^\dagger) is the fermionic annihilation (creation) operator at site j . We consider an initial state $|\Psi(0)\rangle$ consisting of N adjacent fermions on the lattice, corresponding to $|\Psi(0)\rangle = \otimes_{j=1}^N c_j^\dagger |0\rangle$, where $|0\rangle$ is the vacuum of the system (see the sketch in Fig. 1(a)). The case $N = \infty$ corresponds to a single domain wall at site $j = 0$ separating the empty half-chain from the complementary filled one [44, 45].

Ferromagnetic phase for finite N — For finite N , \mathcal{L}_k is the determinant of the matrix $\mathbb{J}_N(k\tau) = [i^{n-m} J_{m-n}(2k\tau)]_{m,n=1\dots N}$, where $J_n(x)$ is the n th Bessel function of the first kind [46]. For large times $k\tau$, the determinant \mathcal{L}_k decays algebraically [46, 47]. According to the mapping discussed above, the energy cost $E(\ell) = -\ln \mathcal{L}(\ell\tau)$ of a domain is, for $\tau \gtrsim 1$, logarithmic in ℓ

$$E(\ell) = c_N \ln \ell + \Delta_N + (N \bmod 2) \ln \cos(2\ell\tau - N\pi/4), \quad (8)$$

where we introduced $c_N = (N^2 + N \bmod 2)/4$. The definition of Δ_N is reported in the Supplemental Material [47, 48]. Introducing the fugacity $y = e^{-\Delta_N}$, the grand canonical partition function of the spin model in Eq. (7) reads

$$\mathcal{Z}_N(z, w) = \frac{w^2 y \Lambda_N(z)}{1 - w y \Lambda_N(z)}, \quad (9)$$

where $\Lambda_N(z)$ is determined in terms of the polylogarithm function [47]. For $w = 1$ and N even, Eq. (9) equals the partition function of the truncated inverse distance squared Ising model (TIDSI) [38] which is parametrised by y and c_N . This system undergoes a mixed-order phase transition from a paramagnetic to a ferromagnetic phase [38–40, 42]. In the quantum picture, however, we consider the partition function $\mathcal{Z}(z, w)$ at $w = -1$. For the spin model, this corresponds to studying the TIDSI model at the (classically forbidden) negative fugacity $-y$.

The leading singularity of \mathcal{Z}_N in Eq. (9) is due to branch points [47, 49, 50]. The integral in Eq. (4) can then be carried out for all N , from which one obtains the leading large- k behaviour of ϕ_k . For $N = 1$, our analysis renders the results of Ref. [13]. For $N > 1$, instead, it gives, up to some oscillating prefactor, $\phi_k \sim \mathcal{L}_k$ and thus the algebraic decay

$$\phi_k \sim k^{-c_N} \quad \text{and} \quad F_k \sim k^{-2c_N}, \quad (10)$$

with logarithmic corrections $\phi_k \sim (\ln k)^n / k^{c_N}$ of all integer orders $n \geq 1$ for $N = 2$ [47]. This algebraic behaviour is consistent with a ferromagnetic, globally ordered phase in the spin model. One can intuitively understand this as a consequence of the logarithmically slow growth of the domain energy $E(\ell)$ in length ℓ , which renders a global ordering thermodynamically favourable in the large k limit and therefore $\phi_k \sim \mathcal{L}_k$. In Fig. 2(a), we show the exact FDRT probabilities F_k for $N = 4$ and 6 [47], with fixed $\tau = 2$, as obtained from the exactly known Loschmidt echo, which are compared with the expected leading algebraic behaviour (10), showing excellent agreement for large k . Figure 2(b) shows that the ratio $F_k / |\mathcal{L}_k|^2$ is well captured by the branch cut asymptotics for intermediate values of $\tau \gtrsim 1.8$ and large values of k .

Paramagnetic phase for $N = \infty$ — For a single domain wall, i.e., for $N = \infty$, the Loschmidt amplitude is exactly given by $\mathcal{L}(\tau) = e^{-\tau^2}$ [44, 46]. In the

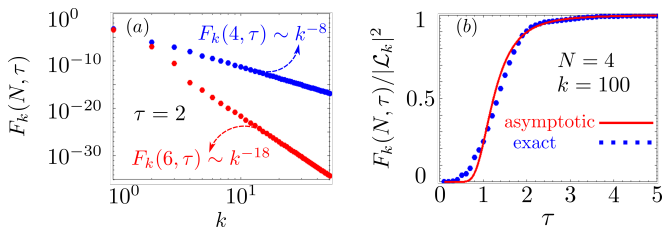


FIG. 2. **Ferromagnetic phase - algebraic decay.** (a) Log-log plot of the first detected return time probability F_k as a function of k for fixed stroboscopic time $\tau = 2$, with $N = 4$ and 6. For sufficiently large $k\tau$, and according to the mapping on the ferromagnetic phase of the spin model, $F_k \sim |\mathcal{L}_k|^2 \sim k^{-2c_N}$ (with $c_4 = 4$ and $c_6 = 9$) decays algebraically upon increasing k . (b) Ratio $F_k/|\mathcal{L}_k|^2$ (blue dots) as a function of τ , for fixed $k = 100$ and $N = 4$ compared with the branch-cut asymptotic (red solid line).

spin model this corresponds to a quadratic energetic cost of a domain, i.e., $E(\ell) = \tau^2 \ell^2$. In order to evaluate $\mathcal{Z}_N(z, w)$ in Eq. (7), we introduce a partial theta function [51] $\Theta_+(z, q) = \sum_{k=1}^{\infty} z^k q^{k^2}$ in terms of which $\hat{\mathcal{L}}(z) = \Theta_+(z, e^{-\tau^2})$. Correspondingly, the grand canonical partition function is

$$\mathcal{Z}_{\infty}(z, w) = \frac{w^2 \Theta_+(z, e^{-\tau^2})}{1 - w \Theta_+(z, e^{-\tau^2})}. \quad (11)$$

As above, we need to understand the analytic properties of $\mathcal{Z}_{\infty}(z, -1)$ for complex z . For all $q \in (0, 1)$, $\Theta_+(z, q)$ is an analytic function of z [52], thus excluding branch cuts. In turn, for $w = -1$, \mathcal{Z}_{∞} has a countable set of poles at the complex roots z_n of $1 + \Theta_+(z_n, q) = 0$ [53]. For $q^{-2} \geq q_{\infty} = 3.23\dots$, these roots are simple, real and negative [54, 55], and they are approximately given, for large n , by $z_n = -q^{1-2n}$ [56]. This implies that for $\tau \geq \tau_c = \sqrt{(\ln q_{\infty})/2} = 0.77\dots$ the contour integral in Eq. (4) is given by the sum over all simple residues which is dominated, for large k , by the the root $z^* = z_1$ closest to the origin. One then finds $\phi_k \sim (z^*)^{-k}$ for $\tau > \tau_c$ with a k -independent prefactor. This exponential decay is shown in Fig. 3(a) for $\tau = 0.8 > \tau_c$. This behaviour corresponds to the paramagnetic phase in the spin model and can therefore be explained with the stronger quadratic growth of $E(\ell)$ upon increasing ℓ , compared to the logarithmic growth (8) for finite N . For $\tau < \tau_c$, the poles of \mathcal{Z}_{∞} are complex conjugate and therefore F_k displays oscillations as a function of k . This is illustrated in Fig. 3(a) for $\tau = 0.1 < \tau_c$. Asymptotically, for large τ , the leading root of $1 + \Theta_+(z, e^{-\tau^2})$ is given by $z^* \approx -e^{-\tau^2} = -\mathcal{L}(\tau)$ such that $F_k \sim |\mathcal{L}(\tau)|^{2k}$, with the proportionality factor approaching 1 as $\tau \gtrsim 1$. The asymptotics of $F_k/|\mathcal{L}_1|^{2k}$ for $\tau > \tau_c$ can be systematically improved by applying Faà di Bruno's theorem [57, 58] to \mathcal{Z}_{∞} , leading to an expansion in the maximal domain length ℓ_M considered [47]. The estimates with $\ell_M = 3$ are compared in Fig. 3(b) with the exact results of $F_k/|\mathcal{L}_1|^{2k}$, showing excellent agreement.

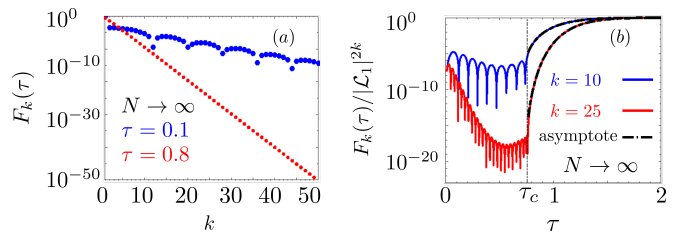


FIG. 3. **Paramagnetic phase - exponential decay.** (a) Log-linear plot of the first detected return time probability $F_k(\tau) \equiv F_k(N = \infty, \tau)$ of the semi-infinite occupied line as a function of k for stroboscopic times $\tau = 0.1$ (top-blue dotted) and 0.8 (bottom-red dashed). F_k decays exponentially in k , according to the mapping to the paramagnetic phase of the spin model. This exponential decay holds for all values of τ . For $\tau < \tau_c = 0.77\dots$, F_k features additional oscillations (blue symbols). (b) Log-linear plot of the ratio $F_k(\tau)/|\mathcal{L}_1|^{2k}$ as a function of τ for fixed values of $k = 10$ and 25. This ratio, for $\tau > \tau_c$, is well approximated by the systematic expansion (dashed-black lines) mentioned in the main text. For $\tau < \tau_c$, instead, the asymptotics break down and $F_k(\tau)$ displays $k - 2$ positive roots as a function of τ .

Phase crossover and ferromagnetic transition—

We investigate here the onset of the ferromagnetic phase in F_k upon increasing k beyond a crossover volume k_{cr} . For sufficiently small $k < k_{cr}$, F_k is in perfect agreement with the paramagnetic behavior observed for $N = \infty$ fermions and predicted by $\mathcal{Z}_{\infty}(k, -1)$ in Eq. (11). Upon increasing k beyond k_{cr} , instead, F_k sharply crosses over into the ferromagnetic behavior predicted by Eq. (9), where $F_k \sim |\mathcal{L}_k|^2$. This crossover is illustrated in Fig. 4(a) for $N = 6$ and $\tau = 1$. Note that, upon increasing τ , the initial exponential decay might not be visible, as it happens in Fig. 2(a) with $\tau = 2$, where only the eventual algebraic behavior is seen. In a complementary way, Fig. 4(b) shows that for a fixed value of $k = 10$, larger values of $\tau > \tau_{cr}$ are needed in order for F_k to be described by the ferromagnetic partition function in Eq. (9).

For large N , this crossover from paramagnetic to ferromagnetic behaviour can be rationalized by studying the scaling limit of the Loschmidt amplitude $\mathcal{L}(\tau)$. Keeping $x = \tau/N$ finite, $\mathcal{L}(\tau)$ satisfies $\lim_{N \rightarrow \infty} N^{-2} \ln \mathcal{L}(Nx) = -f(x)$ where, up to oscillating factors for N odd, $f(x) \approx (\ln x)/4 + 3/8$ for $x \gg 1$ and $f(x) \approx x^2$ for $x \ll 1$ [46]. This fact implies that, upon rescaling the stroboscopic time τ with the number N of fermions, the energy $E(k) = N^2 f(k\tau/N)$ associated to a domain in the spin model may either grow logarithmically or quadratically as a function of k . We conclude that the typical crossover chain volume $(k\tau)_{cr}$, above which F_k decays algebraically, satisfies $(k\tau)_{cr} \sim N$. This linear scaling between space and time follows from the ballistic spreading of free fermions [44, 59–68] and is an intrinsic many-body feature, which enables one to tune the onset of the ferromagnetic decay by scaling the probing time τ according to the number of particles.

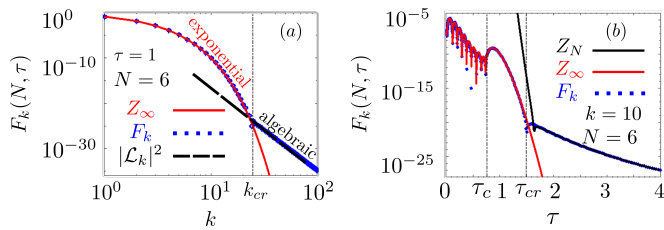


FIG. 4. **Phase crossover.** (a) Log-log plot of the first detection probability $F_k(N, \tau)$ as a function of k for a fixed stroboscopic time $\tau = 1$ and particle number $N = 6$. Upon increasing k , F_k shows a crossover from an exponential-paramagnetic to an algebraic-ferromagnetic decay. In this panel, the crossover occurs at $k = k_{cr} \approx 25$ for $N = 6$, where $k_{cr} \sim N/\tau$. (b) Log-linear plot of $F_k(N, \tau)$ as a function of τ for fixed $k = 10$ and for $N = 6$ fermions. For $\tau < \tau_{cr}$, with $\tau_{cr} \approx 1.5$, F_k (blue dots) follows the behavior of the paramagnetic partition function $|Z_\infty(k, -1)|^2$ (red line), while for $\tau > \tau_{cr}$, $F_k(\tau)$ displays, up to some proportionality factor, the behavior of the ferromagnetic partition function $|Z_N(k, -1)|^2$ (black line). The crossover stroboscopic time scales as $\tau_{cr} \sim N/k$ upon increasing N .

Summary and outlook— We derived exact analytical results for the first detected return time (FDRT) of many-body quantum systems by mapping the FDRT onto the partition function of a classical system of magnetic domains in one spatial dimension. This mapping provides a physical explanation of the rich behavior of the probability of the FDRT which may display an algebraic (ferromagnetic) or an exponential (paramagnetic) decay at long times. Our results are valid for an arbitrarily large number N of particles, including the limit $N \rightarrow \infty$. The onset of the algebraic decay remarkably can be controlled by scaling the stroboscopic time with N , making such a decay accessible already for relatively small times. At larger N the probability of the FDRT becomes rapidly small and its detection would require to devise more efficient detection protocols. For example, one may introduce resetting [22, 24, 25, 69–75] after a sequence of unsuccessful detections. Alternatively, one could consider the first time at which an observable attains a target value for the first time. In this respect, exploring the influence on the FDRT of possibly emerging collective behaviors such as at quantum critical points [76–81] stands as an open problem for further investigation.

Acknowledgements.— The authors would like to thank Eli Barkai for fruitful discussions and helpful comments. BW would like to thank Giorgio Li, Adam Nahum, and Kay Wiese for insightful discussions. BW and AG acknowledge support from MIUR PRIN project “Coarse-grained description for non-equilibrium systems and transport phenomena (CO-NEST)” n. 201798CZL. BW further acknowledges funding from the Imperial College Borland Research Fellowship. GP acknowledges support from the Alexander von Humboldt foundation through a Humboldt research fellowship for postdoctoral researchers.

- [1] R. Shankar, *Principles of Quantum Mechanics*, 2nd ed. (Springer, New York, NY, 1994).
- [2] K. Jacobs, *Quantum measurement theory and its applications* (Cambridge University Press, 2014).
- [3] H.-P. Breuer and F. Petruccione, *The theory of open quantum systems* (Oxford University Press, 2002).
- [4] C. W. Gardiner and P. Zoller, *Quantum Noise: A Handbook of Markovian and Non-Markovian Quantum Stochastic Methods with Applications to Quantum Optics*, 3rd ed., Springer Series in Synergetics (Springer, Berlin Heidelberg, 2010).
- [5] G. R. Allcock, *Ann. Phys.* **53**, 286 (1969).
- [6] N. Kumar, *Pramana* **25**, 363 (1985).
- [7] H. Krovi and T. A. Brun, *Phys. Rev. A* **74**, 042334 (2006).
- [8] F. A. Grünbaum, L. Velázquez, A. H. Werner, and R. F. Werner, *Commun. Math. Phys.* **320**, 543 (2013).
- [9] S. Dhar, S. Dasgupta, and A. Dhar, *J. Phys. A: Math. Theor.* **48**, 115304 (2015).
- [10] S. Dhar, S. Dasgupta, A. Dhar, and D. Sen, *Phys. Rev. A* **91**, 062115 (2015).
- [11] P. Sinkovicz, Z. Kurucz, T. Kiss, and J. K. Asbóth, *Phys. Rev. A* **91**, 042108 (2015).
- [12] H. Friedman, D. A. Kessler, and E. Barkai, *J. Phys. A: Math. Theor.* **50**, 04LT01 (2016).
- [13] H. Friedman, D. A. Kessler, and E. Barkai, *Phys. Rev. E* **95**, 032141 (2017).
- [14] F. Thiel, D. A. Kessler, and E. Barkai, *Phys. Rev. A* **97**, 062105 (2018).
- [15] F. Thiel, E. Barkai, and D. A. Kessler, *Phys. Rev. Lett.* **120**, 040502 (2018).
- [16] F. Thiel, I. Muelem, D. A. Kessler, and E. Barkai, (2019), [arXiv:1909.02114 \[cond-mat, physics:quant-ph\]](https://arxiv.org/abs/1909.02114).
- [17] Q. Liu, R. Yin, K. Ziegler, and E. Barkai, *Phys. Rev. Res.* **2**, 033113 (2020).
- [18] F. Thiel, I. Muelem, D. Meidan, E. Barkai, and D. A. Kessler, *Phys. Rev. Res.* **2**, 043107 (2020).
- [19] F. Thiel and D. A. Kessler, *Phys. Rev. A* **102**, 012218 (2020).
- [20] V. Dubey, C. Bernardin, and A. Dhar, *Phys. Rev. A* **103**, 032221 (2021).
- [21] D. Das and S. Gupta, *J. Stat. Mech.: Theory Exp.* **2022** (3), 033212.
- [22] R. Yin and E. Barkai, *Phys. Rev. Lett.* **130**, 050802 (2023).
- [23] R. Yin and E. Barkai, [arXiv:2301.06100](https://arxiv.org/abs/2301.06100) (2023).
- [24] M. Kulkarni and S. N. Majumdar, [arXiv:2305.15123](https://arxiv.org/abs/2305.15123) (2023).
- [25] P. Chatterjee, S. Aravinda, and R. Modak, [arXiv:2311.09150](https://arxiv.org/abs/2311.09150) (2023).
- [26] R. Yin, Q. Wang, S. Tornow, and E. Barkai, [arXiv:2401.01307](https://arxiv.org/abs/2401.01307) (2024).
- [27] Q. Wang, S. Ren, R. Yin, K. Ziegler, E. Barkai, and S. Tornow, [arXiv:2402.15843](https://arxiv.org/abs/2402.15843) (2024).
- [28] B. Misra and E. G. Sudarshan, *J. Math. Phys.* **18**, 756 (1977).
- [29] C. B. Chiu, E. C. G. Sudarshan, and B. Misra, *Phys. Rev. D* **16**, 520 (1977).
- [30] E. Schrödinger, *Phys. Z* **16**, 289 (1915).
- [31] Q. Liu, D. A. Kessler, and E. Barkai, [arXiv:2401.09810](https://arxiv.org/abs/2401.09810) (2024).
- [32] C. Dittel, N. Neubrand, F. Thiel, and A. Buchleitner,

- Phys. Rev. A **107**, 052206 (2023).
- [33] A. Purkayastha and A. Imparato, Phys. Rev. A **109**, L020202 (2024).
- [34] D. Poland and H. A. Scheraga, J. Chem. Phys. **45**, 1456 (1966).
- [35] D. Poland and H. A. Scheraga, J Chem Phys **45**, 1464 (1966).
- [36] M. E. Fisher, J. Stat. Phys. **34**, 667 (1984).
- [37] C. Richard and A. J. Guttmann, J. Stat. Phys. **115**, 925 (2004).
- [38] A. Bar and D. Mukamel, Phys. Rev. Lett. **112**, 015701 (2014).
- [39] M. Barma, S. N. Majumdar, and D. Mukamel, J. Phys. A: Math. Theor. **52**, 254001 (2019).
- [40] D. Mukamel, Mixed Order Phase Transitions (2023), arxiv:2303.00470 [cond-mat].
- [41] R. J. Harris and H. Touchette, J. Phys. A: Math. Theor. **50**, 10LT01 (2017).
- [42] A. Bar and D. Mukamel, J. Stat. Mech. **2014**, P11001 (2014).
- [43] P. Flajolet and R. Sedgewick, *Analytic Combinatorics*, 1st ed. (Cambridge University Press, 2009).
- [44] J. Viti, J.-M. Stéphan, J. Dubail, and M. Haque, EPL **115**, 40011 (2016).
- [45] L. Wei, R.-A. Pitaval, J. Corander, and O. Tirkkonen, IEEE Trans. Inf. Theory **63**, 2814 (2017).
- [46] P. L. Krapivsky, J. M. Luck, and K. Mallick, J. Stat. Mech. **2018**, 023104 (2018).
- [47] See Supplemental Material at [URL will be inserted by publisher] for the details of the calculations.
- [48] E. W. Barnes, Philos. Trans. R. Soc. A **196**, 265 (1901).
- [49] H. Bateman and A. Erdélyi, *Higher transcendental functions*, California Institute of technology. Bateman Manuscript project (McGraw-Hill, New York, NY, 1953).
- [50] DLMF, *NIST Digital Library of Mathematical Functions*, <https://dlmf.nist.gov/>, Release 1.1.12 of 2023-12-15, f. W. J. Olver, A. B. Olde Daalhuis, D. W. Lozier, B. I. Schneider, R. F. Boisvert, C. W. Clark, B. R. Miller, B. V. Saunders, H. S. Cohl, and M. A. McClain, eds.
- [51] G. E. Andrews, Adv. Math. **41**, 137 (1981).
- [52] V. Kostov, Mat. Stud. **58**, 142 (2023).
- [53] G. H. Hardy, Proc. London Math. Soc. **s2-2**, 332 (1905).
- [54] O. M. Katkova, T. Lobova, and A. M. Vishnyakova, Comput. Methods Funct. Theory **3**, 425 (2004).
- [55] V. P. Kostov and B. Shapiro, Duke Math. J. **162**, 825 (2013).
- [56] J. I. Hutchinson, Trans. Amer. Math. Soc. **25**, 325 (1923).
- [57] H. Gould, *Combinatorial Identities: A Standardized Set of Tables Listing 500 Binomial Coefficient Summations* (Morgantown Printing, Morgantown, 1972).
- [58] L. Comtet, *Advanced Combinatorics* (Springer Netherlands, Dordrecht, 1974).
- [59] T. Antal, Z. Rácz, A. Rákos, and G. Schütz, Phys. Rev. E **59**, 4912 (1999).
- [60] T. Platini and D. Karevski, Eur. Phys. J. B **48**, 225 (2005).
- [61] M. Collura and G. Martelloni, J. Stat. Mech.: Theory Exp. **2014** (8), P08006.
- [62] N. Allegra, J. Dubail, J.-M. Stéphan, and J. Viti, J. Stat. Mech.: Theory Exp. **2016** (5), 053108.
- [63] B. Bertini and M. Fagotti, Phys. Rev. Lett. **117**, 130402 (2016).
- [64] V. Eisler, F. Maislinger, and H. G. Evertz, SciPost Phys. **1**, 014 (2016).
- [65] M. Kormos, SciPost Phys. **3**, 020 (2017).
- [66] G. Perfetto and A. Gambassi, Phys. Rev. E **96**, 012138 (2017).
- [67] M. Ljubotina, S. Sotiriadis, and T. Prosen, SciPost Phys. **6**, 4 (2019).
- [68] G. Perfetto and A. Gambassi, Phys. Rev. E **102**, 042128 (2020).
- [69] B. Mukherjee, K. Sengupta, and S. N. Majumdar, Phys. Rev. B **98**, 104309 (2018).
- [70] A. Riera-Campenya, J. Ollé, and A. Masó-Puigdellosas, arXiv:2011.04403 (2020).
- [71] G. Perfetto, F. Carollo, M. Magoni, and I. Lesanovsky, Phys. Rev. B **104**, L180302 (2021).
- [72] G. Perfetto, F. Carollo, and I. Lesanovsky, SciPost Phys. **13**, 079 (2022).
- [73] X. Turkishi, M. Dalmonte, R. Fazio, and M. Schirò, Phys. Rev. B **105**, L241114 (2022).
- [74] M. Magoni, F. Carollo, G. Perfetto, and I. Lesanovsky, Phys. Rev. A **106**, 052210 (2022).
- [75] S. Belan and V. Parfenyev, New J. Phys. **22**, 073065 (2020).
- [76] A. Lamacraft and P. Fendley, Phys. Rev. Lett. **100**, 165706 (2008).
- [77] S. Groha, F. H. L. Essler, and P. Calabrese, SciPost Phys. **4**, 43 (2018).
- [78] M. Collura and F. H. L. Essler, Phys. Rev. B **101**, 041110 (2020).
- [79] M. Collura, SciPost Phys. **7**, 72 (2019).
- [80] P. Calabrese, M. Collura, G. Di Giulio, and S. Murciano, EPL **129**, 60007 (2020).
- [81] F. Balducci, M. Beau, J. Yang, A. Gambassi, and A. del Campo, arXiv:2307.02524 (2023).

SUPPLEMENTAL MATERIAL

Thermodynamic phases in first detected return times of quantum many-body systems

Benjamin Walter¹, Gabriele Peretto², and Andrea Gambassi³

¹*Department of Mathematics, Imperial College London, London SW7 2AZ, United Kingdom*

²*Institut für Theoretische Physik, Universität Tübingen, Auf der Morgenstelle 14, 72076 Tübingen, Germany*

³*SISSA–International School for Advanced Studies and INFN, via Bonomea 265, 34136 Trieste, Italy*

In this Supplemental Material we provide the details of the calculations and of the results presented in the main text. In particular, in Sec. I, we recall the exact expression of the Loschmidt amplitude of N adjacent fermions on a lattice and of the first detection amplitude ϕ_k . These expressions have been used in the main text to produce the exact numerical data. In Sec. II we discuss the first detection probability F_k in the quantum Zeno regime of very small probing time $\tau \rightarrow 0$. In Sec. III we derive, via an integration in the complex plane, the asymptotic expression in Eq. (10) of the main text for ϕ_k and F_k at large k . In Sec. IV, we eventually detail the derivation of the asymptotic behavior of $F_k(\tau)$ for $N \rightarrow \infty$ and $\tau > \tau_c$ via the Faà di Bruno formula.

I. FIRST-DETECTION AMPLITUDE OF N ADJACENT FREE FERMIONS: EXACT NUMERICAL RESULTS

We consider a system of free fermions evolving on a chain composed by L lattice sites according to the Hamiltonian

$$\mathcal{H} = \gamma \sum_{j=-L/2}^{L/2-1} \left(c_j^\dagger c_{j+1} + c_{j+1}^\dagger c_j \right), \quad (\text{S1})$$

where the operators c_j and c_j^\dagger satisfy the canonical anticommutation relations $\{c_j, c_{j'}^\dagger\} = \delta_{j,j'}$. Here and in the main text we set the hopping amplitude $\gamma = 1$ (as it just provides the timescale of the evolution). We also assume periodic boundary conditions along the chain, i.e., $c_{j+L} = c_j$ and we focus on the limit $L \rightarrow \infty$ of an infinite chain. The initial state of the dynamics $|\Psi(0)\rangle = \otimes_{j=1}^N c_j^\dagger |0\rangle$, where $|0\rangle$ is the empty lattice, consists of N adjacent fermions. A central quantity for the analysis presented in the main text is the Loschmidt amplitude $\mathcal{L}(\tau) = \langle \Psi(0) | U(\tau) | \Psi(0) \rangle$, which gives the probability amplitude that the N fermions get back to the initial state $|\Psi(0)\rangle$ after time τ . In this case, the Loschmidt amplitude can be exactly computed for generic N , as detailed in Refs. [S44, S46]. We report here only the result:

$$\mathcal{L}(\tau) = \begin{cases} \det [i^{m-n} J_{n-m}(2\tau)]_{m,n=1}^N & \text{for } N < \infty, \\ e^{-\tau^2} & \text{for } N = \infty, \end{cases} \quad (\text{S2})$$

where $J_n(t)$ is the n th Bessel function of the first kind. We emphasize that Eq. (S2) is valid in the limit $L \rightarrow \infty$, where the Bessel function $J_{n-m}(\tau)$ emerges as the amplitude of finding a fermion, initially at site m , at site n at time τ . The limiting case $N = \infty$ represents an initial domain-wall state, where half of the chain is initially filled, while the other half is empty. This latter case is discussed in details in Refs. [S44, S45]. For determining the first detection probability (c.f. Sec. III), the asymptotic of the Loschmidt amplitude $\mathcal{L}(\tau)$ for large $\tau \gg 1$ and generic, finite, N will be useful. We report here the corresponding expression, taken from Ref. [S46]:

$$\mathcal{L}(\tau) \simeq \begin{cases} C_N \tau^{-c_N} & \text{for even } N, \\ C_N \cos(2\tau - N\pi/4) \tau^{-c_N} & \text{for odd } N. \end{cases} \quad (\text{S3})$$

We note that, for even N , the Loschmidt amplitude decays monotonically and in an algebraic way for large $\tau \gg 1$, while oscillations are superimposed to the algebraic decay for odd N . In Eq. (S3), we denote by

$$c_N = (N^2 + N \bmod 2)/4 \quad (\text{S4})$$

the exponent of the algebraic decay, while the amplitude C_N is given by $C_N = 2^{\frac{N(N-2)}{4}} \pi^{-\frac{N}{2}} G^2\left(\frac{N+2}{2}\right)$ for even N and $C_N = 2^{\frac{(N-1)^2}{4}} \pi^{-\frac{N}{2}} G\left(\frac{N+1}{2}\right) G\left(\frac{N+3}{2}\right)$ for odd N . In these expressions $G(m)$ denotes Barnes' G function [S48].

In the presence of stroboscopic measurements with probing time τ , the first detection amplitude ϕ_k at time $k\tau$ is constructed from the Loschmidt echo according to Eq. (2). In particular, for any finite k , Eq. (2) implies the quantum renewal equation for ϕ_k [S8, S10, S12]

$$\phi_k = \mathcal{L}_k - \sum_{n=1}^{k-1} \mathcal{L}_n \phi_{k-n}. \quad (\text{S5})$$

Hereafter we adopt the notation $\mathcal{L}_n = \mathcal{L}(n\tau)$ for the sake of brevity. The quantum renewal equation (S5) allows us to compute the first detection amplitude ϕ_k in the presence of stroboscopic measurements from the sole knowledge of the return amplitude \mathcal{L}_k in the absence of measurements. In particular, the first-detection amplitudes ϕ_k , with $k \geq 1$, are recursively obtained from the Loschmidt amplitudes. For example, the first four terms read as

$$\begin{aligned} \phi_1 &= \mathcal{L}_1, \\ \phi_2 &= \mathcal{L}_2 - \mathcal{L}_1^2, \\ \phi_3 &= \mathcal{L}_3 - 2\mathcal{L}_1\mathcal{L}_2 + \mathcal{L}_1^3, \\ \phi_4 &= \mathcal{L}_4 - 2\mathcal{L}_3\mathcal{L}_1 - 2\mathcal{L}_2^2 + 3\mathcal{L}_2\mathcal{L}_1^2 - \mathcal{L}_1^4. \end{aligned} \quad (\text{S6})$$

Upon taking the square modulus, one recovers the exact first-detected return probabilities $F_k = |\phi_k|^2$. For larger values of k , this recursive approach becomes unfeasible. Accordingly, it is more convenient to consider the generating function

$$\hat{\phi}(z) = \sum_{k=1}^{\infty} \phi_k z^k = \frac{\hat{\mathcal{L}}(z)}{1 + \hat{\mathcal{L}}(z)}, \quad \text{with} \quad \hat{\mathcal{L}}(z) = \sum_{k=1}^{\infty} \mathcal{L}_k z^k, \quad (\text{S7})$$

which is written in terms of the generating function $\hat{\mathcal{L}}(z)$ of the measurement-free Loschmidt echo. The first detection amplitude ϕ_k can now be computed from Eq. (S7) by using a computer algebra system to obtain the symbolic expansion of $\hat{\phi}(z)$ in powers of z . The numerical calculation of $\hat{\mathcal{L}}(z)$, required to evaluate $\hat{\phi}(z)$, is performed by truncating the sum which defines $\hat{\mathcal{L}}(z)$ in Eq. (S7) to the first K terms, i.e., $\hat{\mathcal{L}}(z) \approx \hat{\mathcal{L}}_K(z) = \sum_{k=1}^K \mathcal{L}_k z^k$. Powers with $k > K$ in $\hat{\mathcal{L}}(z)$ do not, indeed, contribute to ϕ_K . The latter is therefore exactly computed from the corresponding series expansion at order K of $\hat{\phi}(z)$ from Eq. (S7), with $\hat{\mathcal{L}}(z) \rightarrow \hat{\mathcal{L}}_K(z)$. In this way, we obtain numerically exact data for the first detection probability $F_k = |\phi_k|^2$ as a function of k . These data are then compared with the asymptotic predictions presented in the next sections. The approach described here is computationally feasible on a single computer node for values of K up to $K \approx 500$.

II. SMALL- τ EXPANSION — THE QUANTUM ZENO REGIME

As $\tau \rightarrow 0$, the first-detection return probabilities approach $F_k = \delta_{k,1}$. This can be readily seen because the very definition of $\mathcal{L}(\tau)$ implies that $\lim_{\tau \rightarrow 0} \mathcal{L}(\tau)$ and therefore $\mathcal{L}_k = 1$, for all values of k . This, in turn, yields $\lim_{\tau \rightarrow 0} \hat{\mathcal{L}}(z) = z/(1-z)$ [see Eq. (S7)]. Inserting the latter expression into Eq. (S7), one obtains $\hat{\phi}(z) = z$ and therefore $\phi_k = \delta_{k,1}$. This result simply reflects that the target state $|\Psi(0)\rangle$, which coincides with the initial state, is detected with probability 1 at the first measurement. This is the quantum Zeno effect: under very frequent projective measurements the wavefunction does not evolve from the initial state $|\Psi(0)\rangle$. For small but finite τ , one needs a different approach. As shown in Refs. [S45, S46], the series expansion of $\mathcal{L}(\tau)$ of N adjacent fermions agrees up to order τ^{2N} in τ with the domain wall result of $\mathcal{L}(\tau) = e^{-\tau^2}$ (the two series expansions, in fact, differ starting from order τ^{2N+2}). This means that, at the leading order in τ , the exact Loschmidt amplitudes given in Eq. (S2) has the following expansion: $\mathcal{L}(\tau) = 1 - \tau^2 + \mathcal{O}(\tau^4)$. Summing over all \mathcal{L}_k , this leads to

$$\hat{\mathcal{L}}(z) = \sum_{k=1}^{\infty} \mathcal{L}_k z^k = \frac{z}{1-z} - \tau^2 \text{Li}_{-2}(z) + \mathcal{O}(\tau^4). \quad (\text{S8})$$

Equation (S7) allows one to obtain $\hat{\phi}(z)$ from $\hat{\mathcal{L}}(z)$. Expanding $\hat{\phi}(z)$ at the leading order in τ^2 , one finds

$$\phi(z) = z - \tau^2 \frac{z+z^2}{1-z} + \mathcal{O}(\tau^4) = z - \tau^2(1+z) \sum_{k=1}^{\infty} z^k = z(1-\tau^2) - 2\tau^2 \sum_{k=2}^{\infty} z^k, \quad (\text{S9})$$

from which one deduces $\phi_1 = 1 - \tau^2$ and $\phi_{k \geq 2} = -2\tau^2$. Accordingly, $F_k = 4\tau^2$ for $k \geq 2$, and since $|\mathcal{L}_k|^2 = 1 - 2\tau^2 + \mathcal{O}(\tau^4)$ their ratio has the following expansion:

$$\frac{F_k}{|\mathcal{L}_k|^2} = 4\tau^2 + \mathcal{O}(\tau^4), \quad \text{for } k \geq 2. \quad (\text{S10})$$

We checked numerically Eq. (S10) against the exact evaluation of F_k discussed above and we find that the quantum Zeno prediction reproduces the data well only for $\tau \lesssim 10^{-2}$.

III. ASYMPTOTIC BEHAVIOUR OF THE FIRST DETECTION RETURN PROBABILITY OF N FERMIONS FROM BRANCH CUT INTEGRALS

In this Section, we report the calculation of the large k -behaviour of the first detection amplitude ϕ_k for N adjacent fermions, reported in Eq. (10) of the main text. This expression is obtained by evaluating the complex contour integration [see Eq. (S7)]

$$\phi_k = \oint_C \frac{dz}{2\pi i} \frac{\hat{\phi}(z)}{z^{k+1}}, \quad (\text{S11})$$

with the generating function $\hat{\phi}(z) = \lim_{w \rightarrow -1} \mathcal{Z}_N(z, w)$. Similar calculations have been done in Ref. [S13] in the case of a single particle $N = 1$. Accordingly, in this section, we consider a finite $N \geq 2$. As we explain below, the partition function \mathcal{Z}_N given in Eq. (9) of the main text can be found from Eq. (S7) and from the asymptotic expression of the Loschmidt echo in Eq. (S3). In particular, the moment generating function $\hat{\mathcal{L}}(z)$ of Eq. (S3) reads

$$\hat{\mathcal{L}}(z) = \sum_{k=1}^{\infty} \mathcal{L}_k z^k = y \Lambda_N(z), \quad (\text{S12})$$

where $y = e^{-\Delta_N}$, with $\Delta_N = c_N \ln \tau - \ln C_N$. The definition of Δ_N appears in Eq. (8) of the main text, which simply follows by taking the logarithm of Eq. (S3) with the replacement $\tau \rightarrow \ell\tau$. The constants c_N and C_N have been defined right after Eq. (S3). The function $\Lambda_N(z)$ is readily identified from the definition of the polylogarithm function:

$$\Lambda_N(z) = \begin{cases} \text{Li}_{c_N}(z) & \text{for even } N, \\ \frac{e^{-iN\pi/4} \text{Li}_{c_N}(e^{2i\tau} z) + e^{iN\pi/4} \text{Li}_{c_N}(e^{-2i\tau} z)}{2} & \text{for odd } N \text{ and } \tau \notin \{j\pi/2\}_{j \in \mathbb{N}}, \\ \cos(N\pi/4) \text{Li}_{c_N}((-1)^j z) & \text{for odd } N \text{ and } \tau = j\pi/2, \text{ with } j \in \mathbb{N}. \end{cases} \quad (\text{S13})$$

We recall that the polylogarithm function $\text{Li}_s(z)$ is defined as $\text{Li}_s(z) = \sum_{k=1}^{\infty} z^k / k^s$ for $|z| < 1$, while its definition for $|z| > 1$ is obtained by analytic continuation. From Eq. (S13), we recover the grand-canonical partition function \mathcal{Z}_N given in Eq. (9) of the main text. This partition function features branch-cut singularities, whose number and position depend on the parity of N and on the value of τ , as we discuss in detail in Subsecs. III A, III B, and III C below. On the basis of Eq. (S13), for N odd, we henceforth refer to the case in which τ is an integer multiple of $\pi/2$ (bottom line of Eq. (S13)) as a resonant probing time. When, instead, τ is not an integer multiple of $\pi/2$ (middle line of Eq. (S13)), it will be referred to as non-resonant. The two cases lead to different asymptotics for ϕ_k . Here we anticipate the results of this analysis, i.e., the asymptotic decay of ϕ_k for large k :

$$\phi_k \sim \begin{cases} \frac{y k^{-c_N}}{[1 + y\zeta(c_N)]^2} & \text{even } N \geq 4, \\ \text{Re} \left[\frac{e^{-i(2k\tau - N\pi/4)}}{(1 + yA_+)^2} \right] y k^{-c_N} & \text{odd } N \geq 3 \text{ and } \tau \notin \{j\pi/2\}_{j \in \mathbb{N}}, \\ (-1)^{kj} \frac{\cos(N\pi/4)}{[1 + y\zeta(c_N) \cos(N\pi/4)]^2} y k^{-c_N} & \text{odd } N \geq 3 \text{ and } \tau = j\pi/2 \text{ with } j \in \mathbb{N}, \end{cases} \quad (\text{S14})$$

with $A_+ = [e^{+iN\pi/4} \zeta(c_N) + e^{-iN\pi/4} \text{Li}_{c_N}(e^{+4i\tau})] / 2$ and where $\zeta(s) = \sum_{k=1}^{\infty} k^{-s}$ is the Riemann zeta function. Here, for odd $N \geq 3$, the result for resonant values of $\tau = j\pi/2$ equals the limit of the expression for non-resonant τ as

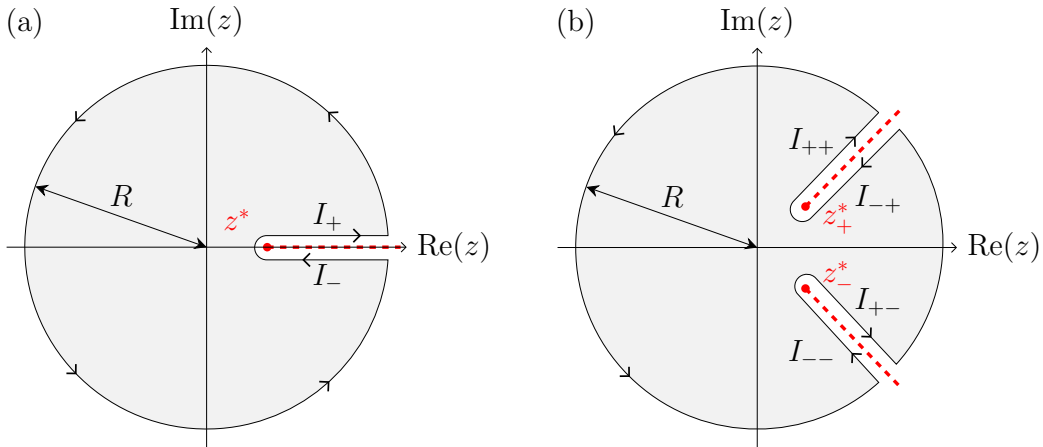


FIG. S1. **Integration path for determining the asymptotic behavior of the first detection amplitude.** In order to evaluate the integral in Eq. (4), with the generating function $\hat{\phi}(z)$ given in Eq. (9), we deform the integration contour in the complex plane around the origin. Depending on the parity of N , and on the value of τ , $\hat{\phi}(z)$ may display either one or two branch cuts. (a) For even N , or odd N but with $\tau = j\pi/2$ for some integer j , the function displays a single branch cut on the positive real line starting at $z^* = 1$. (b) For odd N and generic $\tau \notin \{j\pi/2\}_{j \in \mathbb{N}}$, the function $\hat{\phi}(z)$ displays two branch cuts with branch points at $z_{\pm}^* = e^{\pm 2i\tau}$, which are depicted in the figure.

$\tau \rightarrow j\pi/2$; This is in contrast to what happens for $N = 1$ [S13], where the limit of the expression for non-resonant τ differs from the result corresponding to resonant τ by a factor of two. This fact is further discussed in Sec. III C below. The case $N = 2$ shows a rich behavior since the logarithmic corrections to the algebraic decay are present. For this case we perform an asymptotic expansion of ϕ_k for small y (large probing time τ) and we find, up to order y^3 , that

$$\phi_k \sim k^{-1}[B_0(y) + B_1(y) \ln k + B_2(y) \ln^2 k] + \mathcal{O}(y^4), \quad N = 2. \quad (\text{S15})$$

The expressions of the coefficients $B_0(y), B_1(y), B_2(y)$ are reported further below in Eq. (S32). We see that the expansion to order y^3 introduces logarithmic corrections up to order $\ln^2 k$ in the asymptotic decay of ϕ_k as a function of k . The expansion (S15) can be systematically improved by computing higher orders y^n with $n > 3$, which produce additional logarithmic corrections up to order $\ln^{n-1} k$. One can see that in all the cases $N > 2$, up to some possibly oscillating prefactor, the first detection amplitude ϕ_k decays always algebraically at large k , with $\phi_k \sim k^{-c_N}$. The exponent of this decay is the same as that of the Loschmidt echo in Eq. (S3). Also for $N = 2$, the exponent $k^{-c_2} = k^{-1}$ of the algebraic decay is set by the Loschmidt echo. In the main text, we show a comparison between the asymptotic prediction in Eq. (S14) and the exact numerical data (see Sec. I) finding excellent agreement.

In the following Subsections we provide the details of the derivation of Eq. (S14). In particular, in Subsec. III A, we consider the case of even $N \geq 4$. In Subsec. III B, instead, we present the case $N = 2$ with the ensuing logarithmic corrections. In Subsec. III C, then, we focus on the case with odd $N \geq 3$.

A. Algebraic decay of the first detection return probability for an even number $N \geq 4$ of fermions

We consider here the case in which N is even and larger than or equal to 4. From Eq. (9) of the main text and Eq. (S13), the partition function reads $\mathcal{Z}(z, -1) = y \text{Li}_{c_N}(z) / [1 + y \text{Li}_{c_N}(z)]$. This function displays a single branch cut along $z \in [1, \infty)$, due to the analogous branch cut in $\text{Li}_{c_N}(z)$ on the real axis for $z \in [1, \infty]$ and $c_N \notin \mathbb{Z}$ (in all the calculations, we take the principal value $\text{Arg}(z)$ of the argument of a complex number z in the interval $\text{Arg}(z) \in (-\pi, \pi]$). At $z = 1$, the polylogarithm becomes $\text{Li}_{c_N}(z = 1) = \zeta(c_N)$ which is finite because $c_N = N^2/4 > 1$. The imaginary part of the polylogarithm displays a jump across the cut, with [S49, S50, §1.11.(19)]

$$\text{Im} [\text{Li}_{c_N}(z \pm i0^+)] = \pm \frac{\pi}{\Gamma(c_N)} (\ln z)^{c_N-1}, \quad (\text{S16})$$

while the real part is continuous. Here, $\Gamma(c_N)$ denotes the Euler gamma function. When calculating the complex contour integral in Eq. (S11), the integration contour is deformed in such a way to enclose the branch cut, as shown in

Fig. S1(a). Taking the limit of infinite radius R of the contour, while extending the length of the part of the contour which encloses the branch cut at $z \in [1, \infty)$, the only non vanishing contributions to the integral are provided by the line integrals just above and below the branch cut which we denote by

$$I_{\pm} = \int_1^{\infty} \frac{dz}{2\pi i} \frac{\hat{\phi}(z \pm i0^+)}{(z \pm i0^+)^{k+1}}. \quad (\text{S17})$$

The first-detection amplitude in Eq. (S11) is thus given by

$$\phi_k = I_+ - I_-. \quad (\text{S18})$$

In the subtraction above, all terms which are analytic in z cancel out and one is left with the non-analytic part due to the branch cut, determined by Eq. (S16). Since

$$\hat{\phi}(z) = \frac{\hat{\mathcal{L}}(z)}{1 + \hat{\mathcal{L}}(z)} = 1 - \frac{1}{1 + \hat{\mathcal{L}}(z)} = 1 - \frac{1}{1 + y \text{Li}_{c_N}(z)}, \quad (\text{S19})$$

we can write I_{\pm} in Eq. (S18) as

$$I_{\pm} = \int_1^{\infty} \frac{dz}{2\pi i} (z \pm i0^+)^{-k-1} \left[1 - \frac{1}{1 + y \text{Li}_{c_N}(z \pm i0^+)} \right]. \quad (\text{S20})$$

In the large- k limit, the integral is dominated by the region close to $z = 1$, i.e., close to the branch-cut singularity of the polylogarithm in $z \in [1, \infty]$. In particular, for $z \rightarrow 1^+$, the real part of the polylogarithm approaches $\zeta(c_N)$, while the imaginary part is discontinuous across the cut according to Eq. (S16). One can then simplify the expression of I_{\pm} by expanding the integral at the leading order around $z = 1$ as follows

$$\begin{aligned} I_{\pm} &= \int_1^{\infty} \frac{dz}{2\pi i} \exp[-(k+1) \ln(z \pm i0^+)] \left[1 - \frac{1}{1 + y\zeta(c_N) \pm iy\pi(\ln z)^{c_N-1}/\Gamma(c_N)} \right] \\ &= \int_1^{\infty} \frac{dz}{2\pi i} \exp[-(k+1) \ln z] \left[1 - \frac{1}{1 + y\zeta(c_N)} \pm \frac{iy\pi(\ln z)^{c_N-1}}{\Gamma(c_N)[1 + y\zeta(c_N)]^2} + \dots \right], \end{aligned} \quad (\text{S21})$$

where \dots denotes subleading orders in the expansion in powers of $(\ln z)^{c_N-1}$ around $z = 1$, which we neglect for large k . We then perform the change of variable $\nu = \ln z$:

$$\begin{aligned} I_{\pm} &= \int_0^{\infty} \frac{d\nu}{2\pi i} \exp(-k\nu) \left[1 - \frac{1}{1 + y\zeta(c_N)} \pm \frac{iy\pi\nu^{c_N-1}}{\Gamma(c_N)[1 + y\zeta(c_N)]^2} + \dots \right], \\ &= \frac{1}{2\pi i} \left[\frac{1}{k} \left(1 - \frac{1}{1 + y\zeta(c_N)} \right) \pm \frac{iy\pi k^{-c_N}}{[1 + y\zeta(c_N)]^2} + \dots \right]. \end{aligned} \quad (\text{S22})$$

Inserting the expression in Eq. (S22) into Eq. (S18) it is evident that the contribution coming from the analytic terms in the expansion of the polylog around $z = 1$ cancel out exactly and only the nonanalytic contribution due to the discontinuity in Eq. (S16) across the branch cut remains. This leads to the asymptotic expression for the first detection amplitude

$$\phi_k \sim \frac{yk^{-c_N}}{[1 + y\zeta(c_N)]^2}, \quad (\text{S23})$$

which neglects subleading terms as $k \rightarrow \infty$. This is the result anticipated in Eq. (S14) for even $N \geq 4$. For the first detection probability $F_k = |\phi_k|^2$, the exponent $c_N = N^2/2$ of the decay is compared in Fig. 2(a) of the main text with the exact numerical data. The agreement is excellent and it shows that the approximations introduced above are justified and predict the correct exponent of the algebraic decay of ϕ_k as a function of k . The amplitude of the decay in Eq. (S23), instead, matches the value computed numerically and shown in Fig. 2(b) only for large values of $\tau \gtrsim 1.8$. This is caused by the fact that the asymptotics given in Eq. (S3) (see Ref. [S46]) and used to obtain $\hat{\mathcal{L}}(z)$, Eqs. (S12) and (S13), are valid for $\tau \gg 1$ only.

B. Logarithmic corrections to algebraic decay of first detection return probability of $N = 2$ fermions

In this Subsection we consider separately the case $N = 2$, which is characterized by the fact that the generating function $\phi(z)$ diverges logarithmically at the branch point $z = 1$. This can be seen from Eqs. (S12) and (S13), taking into account that $\text{Li}_1(z) = -\ln(1 - z)$. The generating function for $N = 2$ fermions is therefore

$$\hat{\phi}(z) = 1 - \frac{1}{1 - y \ln(1 - z)}. \quad (\text{S24})$$

As in the case with even $N \geq 4$ discussed in Subsec. III A, the integral over $\phi(z)$ is performed by deforming the contour of integration into a keyhole contour enclosing the single branch cut located at $z \in [1, \infty)$, as shown in Fig. S1(a). The first detection amplitude ϕ_k is again written as in Eq. (S18), with the integrals I_{\pm} given by

$$\begin{aligned} I_{\pm} &= \int_1^{\infty} \frac{dz}{2\pi i} (z \pm i0^+)^{-k-1} \left[1 - \frac{1}{1 - y \ln(1 - z \mp i0^+)} \right] \\ &= \int_1^{\infty} \frac{dz}{2\pi i} \exp[-(k+1) \ln(z \pm i0^+)] \left[1 - \frac{1}{1 - y \ln(1 - z \mp i0^+)} \right] \\ &= \int_1^{\infty} \frac{dz}{2\pi i} \exp[-(k+1) \ln z] \left[1 - \frac{1}{1 - y \ln(|1 - z|) \pm i\pi y} \right] \\ &= \int_0^{\infty} \frac{d\nu}{2\pi i} e^{-k\nu} \left[1 - \frac{1}{1 - y \ln(|1 - e^{\nu}|) \pm i\pi y} \right] \\ &= \int_0^{\infty} \frac{d\nu}{2\pi i} e^{-k\nu} \left[1 - \frac{1}{1 - y \ln \nu \pm i\pi y} + \dots \right] = \frac{1}{2\pi i k} - \int_0^{\infty} \frac{d\nu}{2\pi i} e^{-k\nu} \left[\frac{1}{1 - y \ln \nu \pm i\pi y} + \dots \right]. \end{aligned} \quad (\text{S25})$$

In passing from the second to the third equality we used the expression of the branch-cut discontinuity of the logarithm along the negative real axis $\ln(1 - z \pm i0^+) = \ln(|1 - z|) \pm i\pi$, while $\ln(z \pm i0^+) = \ln z$ since the logarithm is, instead, analytic on the positive real line. In the fourth line we performed the change of variable $z = e^{\nu}$ and we expanded the integrand at the leading order around $\nu = 0$, since in the large- k limit, the integral is dominated by the region around $\nu = 0$. As in the case $N \geq 4$, in the difference in Eq. (S18) only terms originating from the branch-cut discontinuity do not cancel out. Accordingly, we eventually obtain the asymptotic expression for ϕ_k at large k :

$$\phi_k \sim \int_0^{\infty} d\nu e^{-k\nu} \frac{y}{(1 - y \ln \nu)^2 + y^2 \pi^2}. \quad (\text{S26})$$

In order to proceed further from (S26) and determine the logarithmic corrections to the algebraic scaling, we introduce the variable $x = k\nu$:

$$\phi_k \sim \frac{f(\ln k)}{k}, \quad \text{with} \quad f(\ln k) = \int_0^{\infty} dx e^{-x} g_{y,k}(x), \quad \text{where} \quad g_{y,k}(x) = \frac{y}{(1 - y \ln x + y \ln k)^2 + y^2 \pi^2}. \quad (\text{S27})$$

The latter equation clearly shows that the FDRT probability $F_k = |\phi_k|^2$ displays, as a function of k and up to logarithmic corrections, an algebraic decay with exponent $2c_2 = 2$, which is dictated by the asymptotic decay of the Loschmidt echo in Eq. (S3). The logarithmic corrections are given by the function $f(\ln k)$, which we evaluate by expanding its integral expression in powers of $y = C_N \tau^{-c_N}$ [see the definition of y after Eq. (S12)] around $y = 0$, i.e., by considering an expansion for long probing time τ . In particular, from Eq. (S27), we have that:

$$g_{y,k}(x) = y[1 - 2(y \ln k - y \ln x) - (y \ln k - y \ln x)^2 - y^2 \pi^2 + 4(y \ln k - y \ln x)^2] + \mathcal{O}(y^4). \quad (\text{S28})$$

Integrating this expression term by term, we eventually get the series expansion in y of the function $f(\ln k)$ up to third order in y :

$$f(\ln k) = y - 2y^2(\ln k + \gamma_E) + y^3[3 \ln^2 k + 6\gamma_E \ln k + 3(\gamma_E^2 + \pi^2/6) - \pi^2] + \mathcal{O}(y^4). \quad (\text{S29})$$

In the last equation, we used the mathematical identities

$$\int_0^{\infty} dx e^{-x} \ln x = -\gamma_E, \quad \text{and} \quad \int_0^{\infty} dx e^{-x} \ln^2 x = \gamma_E^2 + \pi^2/6, \quad (\text{S30})$$

with $\gamma_E = 0.5772\dots$ the Euler-Mascheroni constant. Plugging Eq. (S29) into Eq. (S27), we eventually get the following asymptotic behavior for the first detection amplitude ϕ_k of $N = 2$ fermions:

$$\phi_k \sim k^{-1}[B_0(y) + B_1(y) \ln k + B_2(y) \ln^2 k] + \mathcal{O}(y^4), \quad (\text{S31})$$

where the coefficients $B_0(y), B_1(y), B_2(y)$ are given by

$$B_0(y) = y - 2y^2\gamma_E + 3y^3(\gamma_E^2 - \pi^2/6), \quad B_1(y) = -2y^2 + 6y^3\gamma_E, \quad \text{and} \quad B_2(y) = 3y^3. \quad (\text{S32})$$

The expressions in Eqs. (S31) and (S32) show that the case $N = 2$ has a more complex asymptotic behavior than for $N \geq 4$. As a matter of fact, for long probing time τ (i.e., small y) one has $B_0 \sim y$ and $B_{1,2} \sim 0$. This implies that for very large τ , all logarithmic corrections are suppressed and one has $\phi_k \sim \mathcal{L}_k = yk^{-c_N}$. This is the same behavior as the one observed in Fig. 2(b) of the main text, where the ratio F_k/\mathcal{L}_k is approximately 1 for large τ . For intermediate values of τ and $N = 2$, however, one observes not only a renormalization of the amplitude B_0 of the algebraic decay, which leads to $F_k/\mathcal{L}_k \neq 1$, but also an unexpected appearance of logarithmic corrections $\sim B_{1,2}$. In Eqs. (S31) and (S32), we see that the expansion up to order y^3 generates logarithmic terms up to order $\ln^2 k$. More generically, the order y^{n+1} of the expansion, with $n \geq 1$, is responsible for the emergence of logarithmic terms of order $\ln^n k$. Higher-order logarithmic corrections with $n > 2$ become significant at increasingly smaller values of k , as τ decreases (while y increases) correspondingly. This is shown in Fig. S2 for $\tau = 10$, where we compare the exact numerical data for the dependence of F_k on k (see Sec. I) with the asymptotic expansion in Eqs. (S31) and (S32). One can see that the asymptotic expansion which includes logarithmic corrections up to $\ln^2 k$ order excellently describes the exact data in the whole range of $k \in [1, 500]$ displayed. In fact, the two curves are barely distinguishable, as small discrepancies emerge only for $k \gtrsim 300$. These discrepancies are caused by higher-order logarithmic corrections and the asymptotic expansion can actually be improved by computing higher-order terms in the expansion in y . For the sake of comparison, in Fig. S2 we also plot the algebraic asymptotics $F_k \sim B_0^2(y)/k^2$ ($B_{1,2} = 0$). The exact data turn out to depart from this algebraic decay already for small values of k , showing that logarithmic corrections have to be accounted for in order to properly describe the dependence on k of the first-detection probability F_k .

We note that for τ values smaller than $\tau = 10$ (used in Fig. S2) the asymptotics (S31) and (S32) is not sufficient to describe the data in the k range shown since higher-order logarithmic corrections $\ln^n k$ ($n \geq 3$) are significant. In these cases, however, one can compare the exact data with the complete asymptotics in Eqs. (S26) and (S27). This comparison shows that Eqs. (S26) and (S27) correctly describe the numerically exact data for F_k as function of k for τ values up to the order of unity $\tau \gtrsim 1$. For smaller $\tau \lesssim 1$, the exact data show oscillations superimposed to a decay as a function of k . We observe that Eqs. (S26) and (S27) do not capture the oscillations, but they, remarkably, still predict with a good accuracy the decay envelope as a function of k . These discrepancies between (S26) and (S27) and the exact data are caused by the fact that the asymptotics (S3), which determines Λ_N in Eq. (S13), does not hold for $\tau \lesssim 1$ (as already commented at the end of Subsec. III A).

C. Algebraic decay of first detection return probability for an odd number $N \geq 3$ of fermions

For odd $N \geq 3$, the generating function $\hat{\phi}(z)$ in Eq. (S7) can be calculated via Eqs. (S12) and (S13). In particular, the function $\Lambda_N(z)$ in the latter displays two branch cuts along

$$z_{\pm 1}(u) = u e^{\pm 2i\tau} \quad \text{with} \quad u \in [1, \infty), \quad (\text{S33})$$

as shown in Fig. S1(b). Importantly, $z_{-1}(1) = z_-^* = e^{-2i\tau}$ is a singular point of the polylogarithm $\text{Li}_{c_N}(e^{2i\tau} z)$, while $z_1(1) = z_+^* = e^{2i\tau}$ is a singular point of the polylogarithm $\text{Li}_{c_N}(e^{-2i\tau} z)$. Note that the two branch cuts above merge into a single branch cut along the real axis whenever the probing time $\tau = j\pi/2$ is resonant (the concept of resonant probing time being defined after Eq. (S13)). Accordingly, it is convenient to discuss the resonant probing time case separately from the non-resonant one.

1. Non-resonant time $\tau \notin \{j\pi/2\}_{j \in \mathbb{N}}$

In order to determine the first-detection amplitudes ϕ_k one has to evaluate the complex integral given in (S11). We deform the integration contour around the origin as illustrated in Fig. S1(b), by shaping it into a double keyhole contour enclosing both branch cuts $z_{\pm}(u)$ [see Eq. (S33)]. The contribution of the arcs of radius R vanishes as $R \rightarrow \infty$

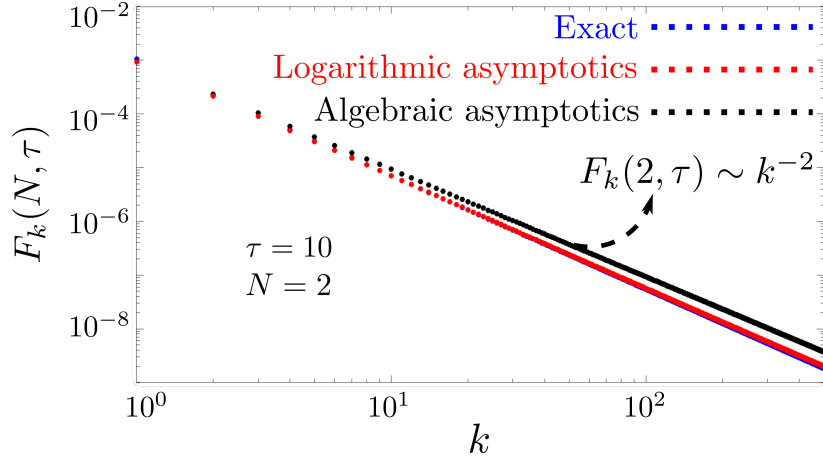


FIG. S2. **Ferromagnetic phase - logarithmic corrections to the FDRT probability for $N = 2$ fermions.** Log-log plot of the first detection probability $F_k(N, \tau)$ as a function of $k \in [1, 500]$ for $N = 2$ fermions and probing time $\tau = 10$. The blue dotted line is the result of an exact numerical calculation, while the red- and black-dotted lines correspond to different asymptotic expressions. In particular, the black-dotted line is the algebraic asymptotics $F_k = B_0^2(y)/k^2$, with the amplitude $B_0(y)$ given in Eq. (S32) and setting $B_{1,2} = 0$ ($y = C_N \tau^{-c_N}$). The red-dotted line, instead, is the asymptotics in Eq. (S31), which account for a logarithmic corrections with coefficients B_0 and $B_{1,2}$ from Eq. (S32). The latter excellently matches the exact data within the range of values of k displayed in the plot. For $k \gtrsim 300$, small discrepancies between Eq. (S31) and the exact data emerge due to higher-order logarithmic corrections $\ln^n k$, with $n \geq 3$.

and therefore one is left with four integrals above and below the two branch cuts. Analogously to Ref. [S13], where the case $N = 1$ is discussed in detail, we introduce

$$\begin{aligned}
I_{\pm, \sigma} &= \frac{1}{2\pi i} \int_1^\infty d(e^{2i\sigma\tau} u) [(u \pm i0^+) e^{2i\sigma\tau}]^{-k-1} \hat{\phi}((u \pm i0^+) e^{2i\sigma\tau}) \\
&= \frac{e^{-2ik\sigma\tau}}{2\pi i} \int_1^\infty du e^{-(k+1)\ln u} \left\{ 1 - \frac{1}{1 + y\Lambda_N((u \pm i0^+) e^{2i\sigma\tau})} \right\} \\
&= \frac{e^{-2ik\sigma\tau}}{2\pi i} \int_0^\infty d\nu e^{-k\nu} \left\{ 1 - \frac{1}{1 + y\Lambda_N((e^\nu \pm i0^+) e^{2i\sigma\tau})} \right\}, \tag{S34}
\end{aligned}$$

where $\sigma = \pm 1$, and where we introduced $\nu = \ln u$, which is analytic along the positive real axis. In the notation $I_{\pm, \sigma}$, the subscript σ indicates which branch cut (S33) the integral refers to, while \pm indicates whether the contour is taken outwards (+) or inwards (-). The four possible terms are shown in Fig. S1(b). By the residue theorem, the integral which determined ϕ_k then equals

$$\phi_k = I_{++} - I_{-+} + I_{+-} - I_{--}. \tag{S35}$$

For large k , the integrand in Eq. (S34) is exponentially suppressed and hence the integral is dominated by the behaviour around $\nu = 0$. In order to study the resulting leading behaviour, we proceed as follows: for odd N , the expression of c_N in Eq. (S4) never renders an integer, i.e., $c_N \notin \mathbb{N}^+ = 1, 2, 3, \dots$ and $c_N > 1$. Accordingly, the polylogarithm can be expanded around $\nu = 0$ as (cf. Ref. [S50])

$$\text{Li}_{c_N}(e^\nu \pm i0^+) = \Gamma(1 - c_N)(-\nu \mp i0^+)^{c_N-1} + \sum_{j=0}^{\infty} \frac{\zeta(c_N - j)}{j!} \nu^j. \tag{S36}$$

The expansion in Eq. (S36) decomposes into a non-analytic contribution, proportional to ν^{c_N-1} , and an analytic part, resulting from the analytic continuation in the complex plane of the Riemann ζ function for $c_N \notin \mathbb{N}$. Accordingly, $\Lambda_N((e^\nu \pm i0^+) e^{2i\sigma\tau})$ (see Eq. (S13)) can be expanded as

$$\Lambda_N((e^\nu \pm i0^+) e^{2i\sigma\tau}) = A_\sigma + \frac{e^{i\sigma N\pi/4}}{2} \Gamma(1 - c_N) (-\nu \mp i0^+)^{c_N-1} + \text{analytic terms } \mathcal{O}(\nu), \tag{S37}$$

where we did not explicitly write down the analytic terms vanishing for $\nu = 0$, and introduced

$$A_\sigma = \frac{1}{2} \left[e^{i\sigma N\pi/4} \zeta(c_N) + e^{-i\sigma N\pi/4} \text{Li}_{c_N}(e^{4i\sigma\tau}) \right]. \quad (\text{S38})$$

One then finds that the four integrals $I_{\pm,\sigma}$ have the following expansions around $\nu = 0$:

$$I_{\pm,\sigma} = \frac{e^{-2ik\sigma\tau}}{2\pi i} \int_0^\infty d\nu e^{-k\nu} \left[1 - \frac{1}{1+yA_\sigma} + e^{i\sigma N\pi/4} \frac{y\Gamma(1-c_N)}{2} \frac{(-\nu \mp i0^+)^{c_N-1}}{(1+yA_\sigma)^2} + \dots \right] \quad (\text{S39})$$

$$= \frac{e^{-2ik\sigma\tau}}{2\pi i} \left[\left(1 - \frac{1}{1+yA_\sigma} \right) \frac{1}{k} + e^{i\sigma N\pi/4} \frac{y\Gamma(1-c_N)}{2(1+yA_\sigma)^2} \int_0^\infty d\nu e^{-k\nu} (-\nu \mp i0^+)^{c_N-1} + \dots \right]. \quad (\text{S40})$$

Here, \dots denotes subleading terms which follow both from the analytic terms in ν from the expansion in Eq. (S37) and from higher-order contributions of the expansion of the non-analytic (logarithmic) part around $\nu = 0$. All these terms are subleading for large values of k . When considering the difference between the integrals done above and below the branch cuts, one finds that the only contributions which do not cancel stem from terms containing non-integer power of ν . In fact, following Eq. (S35), the differences are given by

$$I_{+\sigma} - I_{-\sigma} = \frac{e^{-2ik\sigma\tau+i\sigma N\pi/4}}{2\pi i} \frac{y}{2(1+yA_\sigma)^2} \int_0^\infty d\nu e^{-k\nu} \left(e^{-(c_N-1)\ln(-\nu-i0^+)} - e^{-(c_N-1)\ln(-\nu+i0^+)} \right) + \dots \quad (\text{S41})$$

$$= \frac{e^{-2ik\sigma\tau+i\sigma N\pi/4}}{2\pi i} \frac{y\Gamma(1-c_N)}{2(1+yA_\sigma)^2} \left[e^{-i(c_N-1)\pi} - e^{i(c_N-1)\pi} \right] \int_0^\infty d\nu e^{-k\nu} e^{-(c_N-1)\ln \nu} + \dots \quad (\text{S42})$$

$$= \frac{e^{-2ik\sigma\tau+i\sigma N\pi/4}}{2\pi i} \frac{y\Gamma(1-c_N)}{2(1+yA_\sigma)^2} 2i \sin(\pi(1-c_N)) \Gamma(c_N) k^{-c_N} + \dots \quad (\text{S43})$$

$$= \frac{e^{-2ik\sigma\tau+i\sigma N\pi/4}}{2(1+yA_\sigma)^2} y k^{-c_N} + \dots, \quad (\text{S44})$$

where the last line is simplified using Euler's reflection formula $\Gamma(z)\Gamma(1-z) = \pi/\sin(\pi z)$ (since $z = 1-c_N \notin \mathbb{Z}$). Above we have also neglected subleading terms of order $\mathcal{O}(k^{-c_N-1})$ or higher, which arise when accounting for non-analytic terms of higher-order in ν in the expansion of the integrand in Eq. (S39). Following Eq. (S35), the amplitude is then given by

$$\phi_k \sim \frac{1}{2} \left[\frac{e^{-i(2k\tau-N\pi/4)}}{(1+yA_+)^2} + \frac{e^{i(2k\tau-N\pi/4)}}{(1+yA_-)^2} \right] y k^{-c_N}, \quad (\text{S45})$$

neglecting subleading contributions for large k . Since Eq. (S38) implies that $A_- = (A_+)^*$, the prefactor of the algebraic decay $\sim k^{-c_N}$ above is indeed real and therefore

$$\phi_k \sim \text{Re} \left[\frac{e^{-i(2k\tau-N\pi/4)}}{(1+yA_+)^2} \right] y k^{-c_N}. \quad (\text{S46})$$

This is the result anticipated in Eq. (S14). In the case of odd N , oscillations are superimposed to the asymptotic algebraic decay. The oscillating prefactor of F_k is, up to a k -independent multiplicative constant, determined by the trigonometric functions $\cos^2(2k\tau - N\pi/4)$, $\sin^2(2k\tau - N\pi/4)$ and $\sin(4k\tau - N\pi/2)$ and hence oscillates with a period $\pi/(2\tau)$. The function $F_k k^{2c_N}$ is, specifically, periodic for $k \in \mathbb{N}^+$ only if τ/π is a rational number. Accordingly, for odd N , persistent oscillations are superimposed to the algebraic decay of ϕ_k and thus F_k . The latter is given by $F_k = |\phi_k|^2 \sim k^{-2c_N} = k^{-(N^2+1)/2}$ [see Eq. (S4)], for odd $N \geq 3$, with the exponent $2c_N$ set by the Loschmidt echo asymptotic decay in Eq. (S3). The case $N = 1$, which is discussed in details in Refs. [S13] with calculations similar to those presented in this section, behaves differently. In fact, the first detection probability decays as $F_k \sim k^{-3}$ (still with oscillations of period $\pi/(2\tau)$), while the Loschmidt echo decays with an exponent $2c_1 = 1$. In Fig. S3, we compare the asymptotics in Eq. (S46) with the results of the exact numerical calculation (see Sec. I) and we find excellent agreement as far as the decay exponent $2c_N$ and the amplitude and frequency of the oscillations superimposed to the algebraic decay are concerned.

2. Resonant probing time $\tau = j\pi/2$ with $j \in \mathbb{N}$

We consider here the case in which N is odd and τ is resonant in the sense that $2\tau/\pi$ is an integer j . Then, following Eq. (S13), $\hat{\mathcal{L}}(z) = y \cos(N\pi/4) \text{Li}_{c_N}((-1)^j z)$ has a single branch cut which lies on either the positive or the negative real axis depending on parity of j .

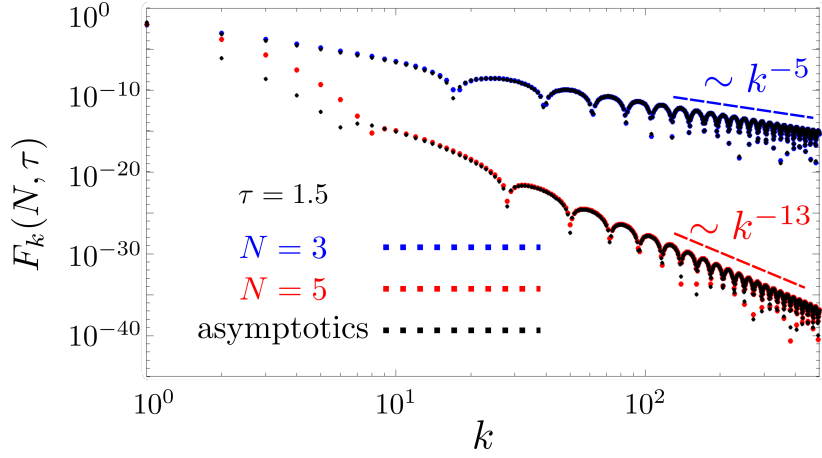


FIG. S3. **Ferromagnetic phase - algebraic decay of the FDRT probability with oscillations for odd particle number.** Log-log plot of the first-detection probability $F_k(N, \tau)$ as a function of $k \in [1, 500]$ for an odd number N of fermions and $\tau = 1.5$. The curves refer to the cases $N = 3$ (top-blue dotted line) and $N = 5$ (bottom-red dotted line). The first-detection probability F_k decays algebraically as a function of k for large values of k , consistently with the mapping to the ferromagnetic phase of the classical spin model. In addition, for odd N , persistent oscillations modulate the amplitude of the algebraic decay. The exact numerical data are compared with the asymptotics $F_k = |\phi_k|^2$ in Eq. (S46) (black-dotted lines for $N = 3$ and 5). These analytical expressions correctly predict both the algebraic decay exponent $2c_N$ [see Eq. (S4), with $2c_3 = 5$ and $2c_5 = 13$] and the amplitude and frequency of the superimposed oscillations.

For even j , it follows from Eq. (S13) that $\hat{\mathcal{L}}(z)$ for this case (odd N and resonant τ) is the same as $\mathcal{L}(z)$ for even N (in which there is no need to distinguish between resonant and non-resonant τ) upon rescaling $y \mapsto y \cos(N\pi/4)$. Accordingly, the resulting ϕ_k follow directly from Eq. (S23) upon replacing y by $y \cos(N\pi/4)$.

For odd j , instead, Eq. (S13) implies that the generating function $\hat{\mathcal{L}}(z)$ with odd N (and resonant τ) maps into $\hat{\mathcal{L}}(z)$ with even N upon simultaneously replacing $y \mapsto \cos(N\pi/4)y$ and $z \mapsto -z$. Inserting this $\hat{\mathcal{L}}(z)$ into Eq. (S7), one finds

$$\phi_k = \frac{1}{2\pi i} \oint \frac{dz}{z^{k+1}} \frac{\hat{\mathcal{L}}(z)}{1 + \hat{\mathcal{L}}(z)} = \frac{(-1)^k}{2\pi i} \oint \frac{dz}{z^{k+1}} \frac{\hat{\mathcal{L}}(-z)}{1 + \hat{\mathcal{L}}(-z)}, \quad (\text{S47})$$

such that, after mapping $z \rightarrow -z$, rescaling y , and multiplying by $(-1)^k$, one recovers the same integral as the one calculated in Eq. (S23). Exploiting these symmetries, and using the results obtained in Eq. (S23), we therefore obtain for odd j

$$\phi_k \sim (-1)^k \frac{\cos(N\pi/4)}{[1 + y\zeta(c_N) \cos(N\pi/4)]^2} y k^{-c_N}. \quad (\text{S48})$$

This is the result anticipated in Eq. (S14). It shows that also for the case of resonant probing time τ , the first detection probability $F_k \sim k^{-2c_N}$ decays algebraically with the same exponent as in the non-resonant case in Eq. (S46). In the former case, however, the algebraic decay is monotonic and no additional oscillations are present.

In passing, we note that the expression in Eq. (S48) can be alternatively obtained by taking the limit $\tau \rightarrow j\pi/2$ of the expression in Eq. (S46), corresponding to a non-resonant τ . This is different to the case $N = 1$, in which by taking the analogous limit of the expression of ϕ_k for non-resonant τ one overestimates the result with resonant τ by a factor of two, as discussed in Ref. [S13]. The reason for this discrepancy is that, in contrast to $N = 1$, none of the two terms in the function (S13) diverge at either branch point for $N \geq 3$. Accordingly, the term A_σ of $\mathcal{O}(\nu^0)$ [see Eq. (S38)] contains contributions from both the terms in (S13) (weighted by a half) which, when taking the limit $\tau \rightarrow j\pi/2$, correctly recover the contribution of a single branch cut. This is not the case for $N = 1$ where $\Lambda_1(z)$ is written in terms of $\text{Li}_{1/2}(z)$ according to Eq. (S13). The polylogarithm $\text{Li}_{1/2}(z)$ diverges in $z = 1$ and therefore the term in Eq. (S13) which remains finite along the branch cut can be neglected as being subleading compared to the other (which is divergent). This causes the constant A_σ to be determined only by the single term divergent in $z = 1$. Consequently, for $N = 1$, ϕ_k in the nonresonant case turns out to eventually overestimate in the limit $\tau \rightarrow j\pi/2$ the resonant first detection amplitude by a factor of 2. In the present case, $N \geq 3$, this does not take place since $\text{Li}_{c_N}(z)$ is always finite in $z = 1$ and the nonresonant result (S48) is obtained continuously as $\tau \rightarrow j\pi/2$ in (S46).

IV. FAÀ DI BRUNO APPROXIMATION FOR THE FDRT PROBABILITY FOR LARGE τ AND $N = \infty$

The generating function $\hat{\phi}(z)$ for the first detection amplitudes $\{\phi_k\}_k$ in Eq. (11) of the main text (see also Eqs. (S7)) can be written as the composition $f(g(z))$ with $f(z) = z/(1+z)$ and $g(z) = \hat{\mathcal{L}}(z) = \Theta_+(z, q = e^{-\tau^2}) = \sum_{k=1}^{\infty} z^k q^{k^2}$. Applying the Faà di Bruno formula for the derivative of a composite function (see, e.g., Ref. [S58]), we can evaluate the $\mathcal{O}(z^k)$ expansion of $\hat{\phi}(z) = f(g(z))$, finding

$$\phi_k = \frac{1}{k!} \left. \frac{d^k}{dz^k} f(g(z)) \right|_{z=0} = \sum_{m_1, \dots, m_k} \frac{1}{m_1!(1!)^{m_1} \dots m_k!(k!)^{m_k}} f^{(m_1 + \dots + m_k)}(g(0)) \prod_{j=1}^k \left(g^{(j)}(0) \right)^{m_j}, \quad (\text{S49})$$

where the sum runs over all partitions $\{m_j\} > 0$ of non-negative integers satisfying $m_1 + 2m_2 + \dots + km_k = k$. This sum is simplified by observing that $g(0) = 0$, $g^{(j)}(0) = j!q^{j^2}$, where $q = e^{-\tau^2}$, and $f^{(n)}(g(0)) = f^{(n)}(0) = (-1)^{n-1}n!$, leading to

$$\begin{aligned} \phi_k &= - \sum_{m_1, \dots, m_k} \frac{1}{\prod_{j'=1}^k m_{j'}!(j')^{m_{j'}}} (-1)^{m_1 + \dots + m_k} (m_1 + \dots + m_k)! \prod_{j=1}^k \left(j!q^{j^2} \right)^{m_j} \\ &= - \sum_{m_1, \dots, m_k} (-1)^{m_1 + \dots + m_k} \frac{(m_1 + \dots + m_k)!}{m_1! \dots m_k!} \prod_{j=1}^k \left(q^{j^2} \right)^{m_j}. \end{aligned} \quad (\text{S50})$$

Each term in the previous sum can be interpreted in terms of the spin model, as discussed in the main text. In fact, one can identify m_j as the number of domains of length j and thus $r = \sum_j m_j$ as the total number of domains in the chain, which has a total volume $k = \sum_j jm_j$. As it can be seen from Eq. (S50), the leading order contribution to ϕ_k is of perturbative order $\mathcal{O}(q^k)$ and arises from the complete partition of the system into domains of length one, corresponding to having $m_1 = k$ and $m_j = 0$ for $j \geq 2$. The exact expression in Eq. (S50) can then be used to determine the subleading corrections to term of order q^k , due to domains of length larger than one. Namely, we perform a perturbative expansion as follows.

We develop a systematic expansion of ϕ_k in q by converting the exact expression (S50) into a perturbative expansion by truncating the power series of $\hat{\mathcal{L}}(z)$ at some finite power K , leading to $g(z) = qz + q^4z^2 + \dots + q^{K^2}z^K$. This means that the summation in Eq. (S50), is restricted to partitions $\{m_j\}$ with $m_{j>K} = 0$. Physically, this corresponds to considering a spin model in which only domains of length up to K are allowed. For $K \geq k$, this restriction does not introduce any error in the computation of ϕ_k as no domain can be larger than the volume k . For $K \leq k-1$, instead, the truncation affects the value of the sum. The associated truncation error is determined by the lowest-order contribution with a single domain of length $K+1$ and then $k - (K+1)$ domains of length 1. Following Eq. (S50), such a configuration is obtained by setting $m_1 = k - (K+1)$, $m_2 = \dots = m_K = 0$, $m_{K+1} = 1$, and is of perturbative order $\mathcal{O}(q^{K^2+K+k})$. This means that, after dividing by the leading q^k term, the perturbative error obtained from truncating the sum at the domain length K is given by $\phi_k/q^k \sim \mathcal{O}(q^{K^2+K})$.

The first non-trivial approximation is for $K = 2$, where

$$\phi_k = - \sum_{m_2=0}^{\lfloor k/2 \rfloor} (-1)^{k-m_2} \frac{(k-m_2)!}{(k-2m_2)!m_2!} q^{k+2m_2} = (-1)^{k-1} q^k \left[\sum_{m_2=0}^{\lfloor k/2 \rfloor} \binom{k-m_2}{m_2} (-q^2)^{m_2} + \mathcal{O}(q^6) \right]. \quad (\text{S51})$$

Hereafter, we denote by $\lfloor x \rfloor$ the greatest integer smaller or equal than x . A serendipitous identity, provided in Eq. (1.60) of Ref. [S57], is

$$\sum_{m=0}^{\lfloor k/2 \rfloor} \binom{k-m}{m} (-1)^m (uv)^m (u+v)^{k-2m} = \frac{u^{k+1} - v^{k+1}}{u-v}. \quad (\text{S52})$$

Setting

$$u = \frac{1 + \sqrt{1-4q^2}}{2}, \quad v = \frac{1 - \sqrt{1-4q^2}}{2}, \quad (\text{S53})$$

one obtains from Eq. (S52) the $K = 2$ Faà-di-Bruno approximation ($q = e^{-\tau^2}$)

$$\phi_k = (-1)^{k-1} e^{-k\tau^2} \left[\frac{\left(1 + \sqrt{1 - 4e^{-2\tau^2}}\right)^{k+1} - \left(1 - \sqrt{1 - 4e^{-2\tau^2}}\right)^{k+1}}{2^{k+1} \sqrt{1 - 4e^{-2\tau^2}}} + \mathcal{O}(e^{-6\tau^2}) \right]. \quad (\text{S54})$$

For $\tau \gtrsim 1$, this expression correctly reproduces the limiting behaviour of $\phi_k = (-e^{-\tau^2})^k$ for large k . Moreover, it also correctly predicts the transition from a monotonic to an oscillatory behavior as a function of τ , shown in Fig. 3(b) of the main text.

An even better asymptotics is obtained by choosing $K = 3$, where the Faà-di-Bruno approximation explicitly reads

$$\phi_k = (-1)^{k-1} q^k \left[\sum_{m_2=0}^{\lfloor k/2 \rfloor} (-1)^{m_2} \sum_{m_3=0}^{\lfloor (k-2m_2)/3 \rfloor} \frac{(k - m_2 - 2m_3)!}{(k - 2m_2 - 3m_3)! m_2! m_3!} q^{2m_2 + 6m_3} + \mathcal{O}(e^{-12\tau^2}) \right]. \quad (\text{S55})$$

We were not able to find an elementary analytic expression of this double sum. We, however, calculated numerically Eq. (S55), which has been used to produce the asymptotic results reported as black dashed lines in Fig. 3(b) of the main text. From this figure, we see that Eq. (S55) already excellently captures the dependence of $F_k(\tau)$ for $\tau > \tau_c$ (with $\tau_c = 0.77\dots$ defined after Eq. (11) of the main text). At τ_c , however, the previously determined asymptotic behavior departs from the numerical data and a sharp transition occurs towards an oscillatory behaviour. This corresponds to the onset of imaginary roots in the partial theta function, as shown also in Fig. 3(a). In particular, Fig. 3(b) shows that $F_k(\tau)$ vanishes at $k - 2$ special values of τ within the interval $(0, \tau_c)$. These roots can be physically understood in terms of the entropically favourable formation of up to $r = 1, 2 \dots k - 1$ longer domains as τ decreases. Due to the quantum nature of $Z_\infty(k, -1)$ in Eq. (6), which requires $w \rightarrow -1$, the associated amplitudes interfere destructively, leading to a vanishing $F_k = |Z_\infty(k, -1)|^2$. Mathematically, these roots can also be understood as follows: expanding Eq. (5) in powers of $q = e^{-\tau^2}$ results in a polynomial with alternating signs and no constant term for which Descartes' rule of signs states that the number of positive real roots is at most $k - 2$. We have done an extensive numerical search of these roots for various values of k , finding that this bound is actually always saturated. However, we cannot currently provide a proof of this fact.